Scaling Behavior of Laser Population Dynamics with Time-Delayed Coupling: Theory and Experiment

Min-Young Kim,[1,2,*] Rajarshi Roy,[1,2,3] Joan L. Aron,[4] Thomas W. Carr,[5] and Ira B. Schwartz[6]
[1]*Department of Physics, University of Maryland, College Park, Maryland 20742, USA*
[2]*Institute for Research in Electronics and Applied Physics, University of Maryland, College Park, Maryland 20742, USA*
[3]*Institute for Physical Science and Technology, University of Maryland, College Park, Maryland 20742, USA*
[4]*Science Communication Studies, Columbia, Maryland 21045, USA*
[5]*Department of Mathematics, Southern Methodist University, Dallas, Texas 75275, USA*
[6]*Code 6792, Plasma Physics Division, Naval Research Laboratory, Washington, D.C. 20375, USA*
(Received 23 August 2004; published 28 February 2005)

We study the influence of asymmetric coupling strengths on the onset of light intensity oscillations in an experimental system consisting of two semiconductor lasers cross coupled optoelectronically with a time delay. We discover a scaling law that relates the amplitudes of oscillations and the coupling strengths. These observations are in agreement with a theoretical model. These results could be applicable to the population dynamics of other systems, such as the spread of disease in human populations coupled by migration.

DOI: 10.1103/PhysRevLett.94.088101 PACS numbers: 87.23.Cc, 42.65.Sf, 89.75.Da

One of the most challenging problems in the study of dynamical systems is that of predicting instabilities and discovering scaling laws that reveal universal characteristics of systems that may initially appear to be very different. An example of such an unexpected correspondence is the connection between the system dynamics of epidemics and lasers, originally introduced by Townes and coworkers to develop an early model of maser dynamics [1,2].

For the convenience of numerical simulation, we consider the scaled equations for a single laser derived in [3]:

$$y' = x(1 + y), \qquad x' = -y - \epsilon x(a + by), \qquad (1)$$

where y is the intensity fluctuation normalized about the steady state level, x is the carrier number fluctuation scaled with respect to the steady state level, and the derivatives are taken with respect to the rescaled time [4]. ϵ is the square root of the ratio of the photon lifetime, τ_p, to the carrier lifetime, τ_c. a and b are parameters defined in terms of the pump rate, gain coefficient, and lifetimes τ_p and τ_c. These equations are analogous to the scaled equations for a single population model of epidemics [5].

We explore a system of two lasers with an optoelectronic coupling scheme where the output intensity of each laser modulates the pump current of the other laser. Passive nonlinear optical media [6] and single laser oscillators with instabilities induced by time-delayed feedback [7,8] have been studied for at least two decades. Previous theoretical studies of globally coupled nonlinear oscillators with time-delayed coupling [9–11] have examined their dynamics and synchronization as a function of coupling strength but do not include the relaxation dynamics of populations with different time scales of decay.

In our experiment, the light emitted from each laser diode (LD) passes through an optical fiber and is monitored by a photodiode detector (PD) whose ac signal (V) is amplified or attenuated and then negatively fed back to the modulation input of the counterpart laser (Fig. 1). The delay in the feedback loop can be easily adjusted by inserting optical fibers of different lengths. The delay time from one laser to the other is fixed at about ~35 ns, which is much longer than the characteristic relaxation

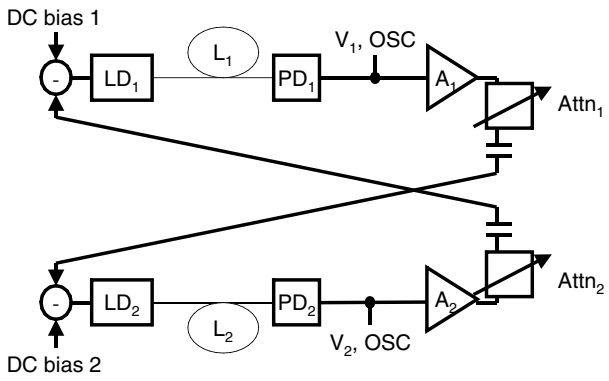

FIG. 1. Schematic diagram of the cross-coupled laser experiment with delayed negative optoelectronic feedback: LD_1 and LD_2, laser diodes; PD_1 and PD_2, photodiodes; L_1 and L_2, optical fibers; OSC, oscilloscope; V_1 and V_2, photodiode output voltages; A_1 and A_2, electronic amplifiers; $Attn_1$ and $Attn_2$, variable electronic attenuators. The thin lines indicate the optical signal path through the fiber and the thick lines indicate the electronic signal path through transmission cables.

oscillation time of the laser dynamics, i.e., ~2–3 ns. The coupling strengths, d_1 (from LD_1 to LD_2) and d_2 (from LD_2 to LD_1), can be controlled separately with variable attenuators in the electronic signal path [12]. All the parameters for the coupled lasers are matched as closely as possible.

Since a signal proportional to the light intensity fluctuations of one laser is fed back to the modulation input of the other laser, the coupling terms are added to the pump rates of each laser. Denoting x_i and y_i ($i = 1, 2$) as the normalized intensity fluctuations and the scaled carrier number fluctuations, respectively, for each laser, the resulting coupled scaled equations for two identical lasers are

$$\begin{aligned} y_1' &= x_1(1 + y_1), \\ x_1' &= -y_1 - \epsilon x_1(a + by_1) - \epsilon\delta_2 y_2(t - \tau), \\ y_2' &= x_2(1 + y_2), \\ x_2' &= -y_2 - \epsilon x_2(a + by_2) - \epsilon\delta_1 y_1(t - \tau). \end{aligned} \tag{2}$$

The coupling constants δ_1 and δ_2 are proportional to the coupling strengths d_1 and d_2 from the experiments.

The coupling strength d_2 is increased for a fixed value of the coupling strength d_1 in experiments. For weak coupling, both lasers show noisy fluctuations of their intensities. As the coupling strength d_2 is made stronger, the emergence of sinusoidal oscillations of the laser outputs is observed, with amplitude that grows with the coupling strength. It is seen that the oscillating signals from each laser are in phase and that the period of the oscillations is double the delay time, i.e., ~70 ns. Intuitively, when the light intensities of both lasers stay high during half of the oscillation period, the output of both will be reduced by the feedback after the propagation time delay and stay low for the rest of the oscillation. Then after another propagation delay time has elapsed, the output of both will increase and stay high. Therefore, in-phase oscillations with a period of twice the time delay become stable.

In Fig. 2(a), the amplitude of the signal measured by PD_2 versus the coupling strength d_2 is shown for different values of the coupling strength d_1 [13]. Note that even when the coupling in one direction is weak, the system starts oscillating if the coupling in the other direction is strong enough. To obtain a quantitative relationship between the coupling strengths at the onset of the oscillations, we plotted values of $\log_{10}(d_1)$ and $\log_{10}(d_2)$ at the emergence of the oscillations and found that these points fall on a straight line, satisfying a linear relation given by

$$\log_{10}(d_1) + \log_{10}(d_2) = \log_{10}(d_1 d_2) = c, \tag{3}$$

as shown in Fig. 2(b), where $c \sim 0.1$. A condition for the onset of the oscillation, therefore, is that the product of d_1 and d_2 increases through a critical constant, i.e., $d_1 d_2 = 10^{0.1} = 1.3$, in our case.

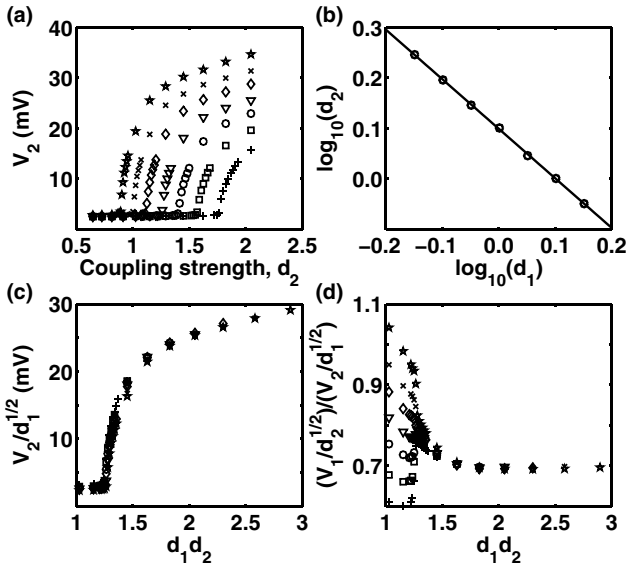

FIG. 2. Experimental observations and analysis. (a) Plot of intensity oscillation amplitude measured by PD_2, V_2, versus coupling strength d_2 for different coupling strengths d_1. Plus signs show the amplitude for $d_1 = 0.71$, squares for $d_1 = 0.80$, circles for $d_1 = 0.89$, triangles for $d_1 = 1.00$, diamonds for $d_1 = 1.12$, crosses for $d_1 = 1.26$, and stars for $d_1 = 1.42$. (b) Plot of $\log_{10}$(coupling strength d_2) vs $\log_{10}$(coupling strength d_1) at the emergence of oscillations. The line shows the best-fit linear model. (c) Rescaled intensity amplitudes, $V_2/\sqrt{d_1}$, versus the product of coupling strengths ($d_1 d_2$), showing data collapse. (d) Plot of the ratio of the rescaled amplitudes $(V_1/\sqrt{d_2})/(V_2/\sqrt{d_1})$ vs ($d_1 d_2$).

There arises the question of whether we can discover a scaling relationship between the amplitude of the signals and the product of the coupling strengths $d_1 d_2$ of the two lasers. When we plot [Fig. 2(c)] the rescaled amplitude of oscillations $V_2/\sqrt{d_1}$ versus ($d_1 d_2$), the individual curves corresponding to different coupling strengths d_1 in Fig. 2(a) collapse to a single curve. A similar collapse is seen for $V_1/\sqrt{d_2}$ vs ($d_1 d_2$). Figure 2(d) shows the ratio of rescaled amplitudes $(V_1/\sqrt{d_2})/(V_2/\sqrt{d_1})$ vs ($d_1 d_2$). When the product ($d_1 d_2$) increases beyond the critical value of 1.3, the ratio converges to a constant and oscillations appear in both systems. This result implies that there exists, to a good approximation, a single function that determines the amplitudes of oscillations in both lasers for given coupling strengths.

Numerical simulations and stability analysis were carried out on the cross-coupled laser model using Eq. (2). The order of the delay time was assumed to be comparable to that of the carrier lifetime. The stability analysis applied near the onset of the oscillations shows that in-phase oscillations with a period of twice the delay time are one of several possible stable solutions. At the onset point, the product of coupling constants satisfies $\delta_1 \delta_2 \sim$ const.

Figure 3(a) shows the amplitude of normalized intensity fluctuations y_2 versus coupling constant δ_2 for different

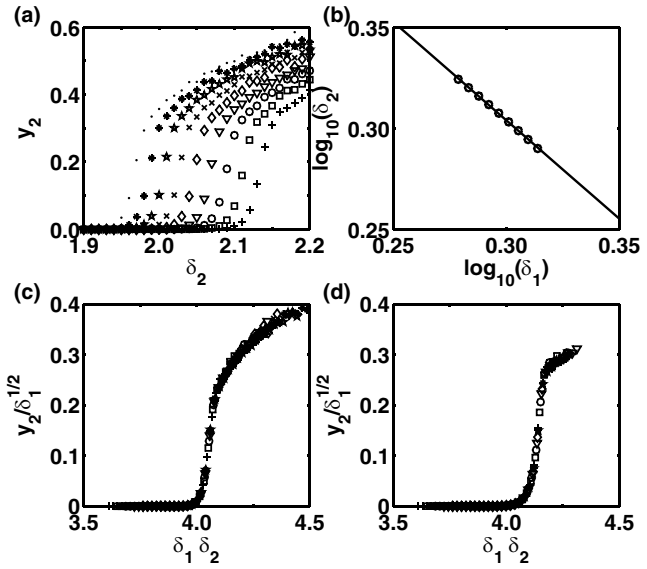

FIG. 3. Numerical computations. (a) Plot of amplitude of the intensity fluctuations normalized to steady state level y_2 versus coupling constant δ_2 for different coupling constants δ_1. Plus signs show the amplitude for $\delta_1 = 1.90$, squares for $\delta_1 = 1.92$, circles for $\delta_1 = 1.94$, triangles for $\delta_1 = 1.96$, diamonds for $\delta_1 = 1.98$, crosses for $\delta_1 = 2.00$, stars for $\delta_1 = 2.02$, asterisks for $\delta_1 = 2.04$, and points for $\delta_1 = 2.06$. (b) Plot of $\log_{10}(\delta_2)$ versus $\log_{10}(\delta_1)$ at the emergence of oscillations. The line shows the best-fit linear model. (c) Plot of rescaled variable $y_2/\sqrt{\delta_1}$ versus the product of the coupling constants $\delta_1\delta_2$, showing the data collapse. The values of the parameters used are $a = 2$, $b = 1$, $\epsilon = \sqrt{0.001}$, and $\tau = 30$ in dimensionless units. (d) The same as (c) with $\tau = 150$. The same marker types are used for same δ_1 values in (a), (c), and (d).

values of coupling constant δ_1 in the numerical computations. The linear relationship between $\log_{10}(\delta_2)$ and $\log_{10}(\delta_1)$ at the emergence of oscillations is shown in Fig. 3(b). In Figs. 3(c) and 3(d), the rescaled amplitude is plotted versus the product of the coupling constants, $\delta_1\delta_2$. The scaling property of the cross-coupled system can be seen very clearly in these figures, which display a data collapse similar to Fig. 2(c), for two values of the delay time, $\tau = 30$ and $\tau = 150$, in dimensionless time units. We thus find that the scaling is preserved for a wide range of ratios of the delay time to the relaxation oscillation period. The ratio of the rescaled amplitudes was found to be unity in the simulations, i.e.,

$$\frac{y_2}{\sqrt{\delta_1}} = \frac{y_1}{\sqrt{\delta_2}} = 1. \tag{4}$$

The experimental observations of cross-coupled lasers demonstrate more complex behavior as shown in Fig. 2(d), since differences between the lasers and detectors, as well as spontaneous emission noise levels, were not accounted for by the model.

With the parameter values used for Fig. 3, the dynamics observed are a combination of the relaxation oscillations and the oscillations induced by delayed coupling. For values of $\delta_1\delta_2$ larger than shown in the figure, the intensity time series is no longer periodic and shows more complex patterns.

The period of oscillations observed in the experiments is sensitive to the bandwidth limitation of the electronic components. When a low pass filter is incorporated into the numerical model, we can observe different periodicities of the oscillations that depend on the cutoff frequency of the filter.

In summary, we have studied the influence of asymmetric coupling strengths on the onset of light intensity oscillations in an experimental system consisting of two semiconductor lasers cross coupled optoelectronically with a time delay. Oscillations occur if the product of the coupling strengths is above a critical value. We have discovered a scaling law that relates the amplitude of oscillations and the product of coupling strengths. These observations are consistent with the theoretical model presented here.

These studies were motivated by the formal correspondences between a class of epidemic models and a class of the laser models [5], which are shown in Table I. What are the epidemiological implications of our observations? The inclusion of an effective delay in the transmission of disease between populations possibly explains some of the interesting dynamical phenomena observed for disease epidemics, including long interepidemic periods and in-phase oscillations of incidence [17,18]. For example, more rapid modes of transportation are thought to be important

TABLE I. Correspondences between a single population epidemic model and a standard laser model.

Description of dynamical variables and parameters	Epidemic model [14,15]	Laser model [16]
Slow dynamical variable	S, susceptible population	N, carrier number
Fast dynamical variable	I, infective population	I, photon number
Source term	ν, susceptible input rate	P, pump rate
Nonlinear coupling	κ, contact rate	g, gain coefficient
Governing equations[a]	$dI/dt = (\alpha(\mu + \gamma))\kappa IS - (\mu + \alpha)I$	$dI/dt = gIN - \tau_p^{-1}I$
	$dS/dt = \nu - \mu S - \kappa IS$	$dN/dt = P - \tau_c^{-1}N - gIN$

[a]In these equations, μ is the death rate, α^{-1} is the average latent period, γ^{-1} is the average infectious period, τ_c is the carrier lifetime, and τ_p is the photon lifetime.

in increasing the frequency of dengue epidemics in the late twentieth century [19].

We acknowledge support from the U.S. Center for Army Analysis and the U.S. Office of Naval Research.

*Electronic address: mmyykim@glue.umd.edu

[1] C. H. Townes, *How the Laser Happened* (Oxford University Press, New York, 1999), p. 84.

[2] K. Shimoda, H. Takahasi, and C. H. Townes, J. Phys. Soc. Jpn. **12**, 686 (1957).

[3] T. W. Carr, L. Billings, I. B. Schwartz, and I. Triandaf, Physica (Amsterdam) **147D**, 59 (2000); I. B. Schwartz and T. Erneux, SIAM J Appl. Math. **54**, 1083 (1994).

[4] The dimensionless time used in the equations is scaled so that $t[\text{dimensionless}] = 2\pi t_{\text{phy}}/T_{\text{rel}}$, where t_{phy} is the real time in seconds and T_{rel} is the period of the relaxation oscillations in seconds.

[5] L. Billings, E. Bollt, D. Morgan, and I. B. Schwartz, in *Proceedings of the Fourth International Conference on Dynamical Systems and Differential Equations, Wilmington, 2002* (American Institute of Mathematical Sciences, Springfield, 2003), p. 122.

[6] H. Nakatsuka, S. Asaka, H. Itoh, K. Ikeda, and M. Matsuoka, Phys. Rev. Lett. **50**, 109 (1983).

[7] F. T. Arecchi, G. Giacomelli, A. Lapucci, and R. Meucci, Phys. Rev. A **43**, 4997 (1991).

[8] J. N. Blakely, L. Illing, and D. J. Gauthier, IEEE J. Quantum Electron. **40**, 299 (2004).

[9] Y. Kuramoto, *Chemical Oscillations, Waves, and Turbulence* (Springer-Verlag, Berlin, 1984).

[10] H. G. Schuster and P. Wagner, Prog. Theor. Phys. **81**, 939 (1989).

[11] M. K. S. Yeung and S. H. Strogatz, Phys. Rev. Lett. **82**, 648 (1999).

[12] The ac-coupled signal from each photodiode is measured by the oscilloscope so that the voltage output V is proportional to the fluctuations of the light intensity. The 3 dB cutoff frequencies of the photodiodes are 30 kHz and 1 GHz. Each laser is biased slightly above the threshold; i.e., $P_0 \sim 1.02P_{\text{th}}$ with temperature stabilized to 0.01 °C. The open loop voltage gains d_1 and d_2 determine the coupling strengths for the two lasers.

[13] For each set of parameters (d_1, d_2), the time series is recorded for time windows of 11 000 delay times, i.e., 0.4 ms, and is divided into ten subwindows. We calculate the standard deviation of the signal in each subwindow and use the average of the standard deviations as the signal amplitude in Fig. 2.

[14] R. M. Anderson and R. M. May, *Infectious Diseases of Humans* (Oxford University Press, New York, 1991).

[15] I. B. Schwartz and H. L. Smith, J. Math. Biol. **18**, 233 (1983).

[16] G. P. Agrawal and N. K. Dutta, *Semiconductor Lasers* (Van Nostrand Reinhold, New York, 1993), Chap. 6.

[17] A. D. Cliff, P. Haggett, and M. Smallman-Raynor, *Measles: An Historical Geography of a Major Human Viral Disease from Global Expansion to Local Retreat, 1840–1990* (Blackwell Publishers, Oxford, 1994).

[18] D. A. T. Cummings *et al.*, Nature (London) **427**, 344 (2004).

[19] D. J. Gubler, Clin. Microbiol. Rev. **11**, 480 (1998); D. J. Gubler, Trends Microbiol. **10**, 100 (2002).